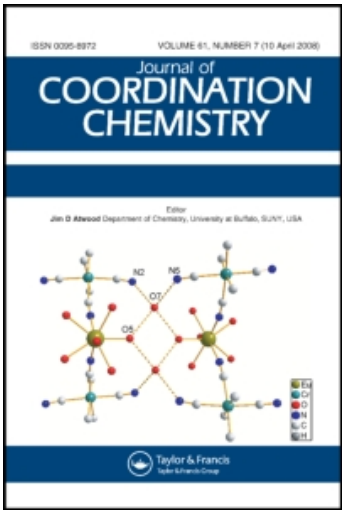

Journal of Coordination Chemistry
Publication details, including instructions for authors and subscription information:
http://www.informaworld.com/smpp/title~content=t713455674

Two organic-inorganic hybrid compounds constructed from 12-tungstovanadate and bipyridine

Ming-Xing Yang[ab]; Shen Lin[ab]; Xiao-Hua Chen[ab]; Ming-Hong Luo[a]; Jiao-Hua Liu[a]
[a] College of Chemistry and Material Science, Fujian Normal University, Fuzhou 350007, P.R. China [b] State Key Laboratory of Structural Chemistry, Fujian Institute of Research on the Structure of Matter, Chinese Academy of Sciences, Fuzhou 350002, P.R. China

First published on: 19 November 2009

To cite this Article Yang, Ming-Xing , Lin, Shen , Chen, Xiao-Hua , Luo, Ming-Hong and Liu, Jiao-Hua(2010) 'Two organic-inorganic hybrid compounds constructed from 12-tungstovanadate and bipyridine', Journal of Coordination Chemistry, 63: 3, 406 — 417, First published on: 19 November 2009 (iFirst)
To link to this Article: DOI: 10.1080/00958970903431704
URL: http://dx.doi.org/10.1080/00958970903431704

Journal of Coordination Chemistry
Vol. 63, No. 3, 10 February 2010, 406–417

Taylor & Francis
Taylor & Francis Group

Two organic–inorganic hybrid compounds constructed from 12-tungstovanadate and bipyridine

MING-XING YANG†‡, SHEN LIN*†‡, XIAO-HUA CHEN†‡, MING-HONG LUO† and JIAO-HUA LIU†

†College of Chemistry and Material Science, Fujian Normal University, Fuzhou 350007, P.R. China
‡State Key Laboratory of Structural Chemistry, Fujian Institute of Research on the Structure of Matter, Chinese Academy of Sciences, Fuzhou 350002, P.R. China

(*Received 29 April 2009; in final form 12 August 2009*)

Two rare 12-tungstovanadate-bipyridine inorganic–organic hybrid compounds, $[VW_{12}O_{40}]\cdot 2(4,4'\text{-}H_2bipy)\cdot 2H_2O$ (**1**) and $[VW_{12}O_{40}]\cdot 4(2,2'\text{-}Hbipy)$ (**2**), have been hydrothermally synthesized and structurally characterized by single-crystal X-ray diffraction and IR analysis. In **1**, a 2-D supramolecular architecture is formed by hydrogen-bonding between $[VW_{12}O_{40}]^{4-}$ and bipy. Compound **1** shows good activity for photocatalytic reduction of rhodamine B in a liquid–solid system. The electrochemical and electrocatalytic properties of 2-bulk carbon paste electrode modified with **2** were investigated by cyclic voltammetry.

Keywords: Supramolecular architectures; Polyoxotungstates; Hydrothermal synthesis; Catalytic activities

1. Introduction

Polyoxometalates (POMs) are a versatile family of metal-oxide clusters with elegant structural and physicochemical properties [1–4] and have been employed as inorganic building blocks for construction of organic–inorganic hybrid materials. In particular, the Keggin POMs are very flexible and can be finely tuned at the molecular level to promote a variety of applications in catalysis, magnetism, electric conductivity, and medicine [5–7]. Their photocatalytic and electrocatalytic properties have attracted attention since they show good properties in photocatalytic detoxification [8–10], electrochemical sensors, and fuel cells [11–13]. Insoluble organic–inorganic hybrid metal oxides based on Keggin POMs are used as catalysts and present three advantages for potential applications. First, they are an environment-friendly catalyst, particularly when applied to ''green technology'' or remediation to clean polluted segments of the environment. Second, they are easily synthesized such that Keggin POMs and their derivatives have a prominent place in POM [14–22]. Third, insolubility can be considered for recycling [23].

*Corresponding author. Email: shenlin@fjnu.edu.cn

Journal of Coordination Chemistry
ISSN 0095-8972 print/ISSN 1029-0389 online © 2010 Taylor & Francis
DOI: 10.1080/00958970903431704

Among Keggin heteropolytungstate organic–inorganic hybrids $[XW_{12}O_{40}]^{n-}$ (X = P [5, 14–17], Si [18–20], etc.) are common. However, a few Keggin compounds of $[VW_{12}O_{40}]^{n-}$ and its derivatives have been reported: $[VW_{12}O_{40}][VO_2Ag(phen)_3]_2$ [21], $[Me_4N]_7[VW_{12}O_{40}]\cdot 15H_2O$ [22], $(C_2N_2H_{10})_2[VW_{11}V_1O_{40}]\cdot 6H_2O$ [24], and $[N(CH_3)_4]_4$ $[VW_{11}V_1O_{40}]\cdot 4\text{-}5H_2O$ [25]. Neutral *N*-donor ligands usually lead to formation of metal–organic complexes or cation segments which might easily bond to the POM anion building blocks to form inorganic–organic hybrid compounds. Hence, pyridine or bipyridine ligands were considered in synthetic efforts for new organic–inorganic hybrid metal oxide compounds. Although photo- and electro-catalytic properties of compounds based on $[XW_{12}O_{40}]^{n-}$ (X = P, Si, etc.) have been extensively studied, no studies of compounds containing Keggin 12-tungstovanadate have been done. As an extension of the above work, herein we report the syntheses, structures and properties of two Keggin 12-tungstovanadate organic–inorganic hybrid compounds $[VW_{12}O_{40}]\cdot 2(4,4'\text{-}H_2bipy)\cdot 2H_2O$ (**1**) and $[VW_{12}O_{40}]\cdot 4(2,2'\text{-}Hbipy)$ (**2**). In **1**, a 2-D supramolecular architecture is formed by tricentered hydrogen-bonding and common hydrogen-bonding between protonated H_2bipy ligands and $[VW_{12}O_{40}]^{4-}$. Compound **1** exhibits good photocatalytic activity for decolorization of rhodamine B (RB) solution and **2** shows electrocatalytic activity for reduction of hydrogen peroxide.

2. Experimental

2.1. *Material and instrumentation*

All chemicals were purchased from commercial sources and used without purification. Vanadium and tungsten were determined on a Perkin–Elmer Optima 3300DV inductively coupled plasma spectrometer. The elemental analyses (C, H, and N) were done on an Elementar Vario EL III analyzer. The electron paramagnetic resonance (EPR) spectrum on a crystalline solid at 100 K was obtained on a Bruker EMX-10/12 diffractometer. IR spectra were recorded with a NICOLET-5700 FT-IR spectrophotometer from 400 to 4000 cm^{-1} using a KBr pellet. Thermogravimetric analysis (TGA) was carried out on a METTLER TGA/SDTA851 instrument from 35°C to 900°C with a heating rate of 10°C min^{-1}. The absorbance of RB was measured on a Spectrum lab 22PC at 554 nm. Cyclic voltammetry measurements were carried out on a CHI 660B electrochemical station using a conventional three-electrode single compartment cell at room temperature. The working electrode was a modified carbon paste electrode (CPE). Platinum gauze was used as the counter electrode and Ag/AgCl was used as the reference electrode.

2.2. *Synthesis of 1 and 2*

A mixture of $H_3[PW_{12}O_{40}]\cdot H_2O$, V_2O_5, 4,4′-bipy, and H_2O in a molar ratio 1 : 1 : 1.84 : 669 was stirred for 30 min, then sealed in an 18 mL Teflon-lined reactor and heated at 160°C for 4 days. Yellow block crystals of **1** were obtained, filtered, washed with water and dried at room temperature. Anal. Calcd for **1** (%): C, 7.39; H, 0.74; N, 1.72; W, 67.88; V, 1.567. Found : C, 7.45; H, 0.75; N, 1.70; W, 67.61; V, 1.748.

Table 1. Crystallographic data.

	1	2
Emperical formula	$C_{20}H_{24}N_4O_{42}VW_{12}$	$C_{40}H_{36}N_8O_{40}VW_{12}$
Formula weight	3249.57	3525.91
Crystal system	Monoclinic	Triclinic
Space group	*P 2(1)/n*	*P-1*
Unit cell dimension (Å, °)		
a	11.530(3)	11.161(2)
b	12.109(3)	12.291(3)
c	17.342(4)	13.111(3)
α	90	68.55(3)
β	103.466(4)	84.93(3)
γ	90	67.80(3)
Volume (Å^3), *Z*	2354.6(10), 2	1547.3(5), 1
F(000)	2838	1563
Calculated density (mg cm^{-3})	4.583	3.784
Absorption coefficient (mm^{-1})	29.482	22.448
θ range for data collection (°)	2.07–27.48	2.04–27.48
R_{int}	0.0462	0.0582
No. of data collected	17,895	11,868
No. of unique data	5384	6976
No. of observed	4530	4853
No. of variables	384	476
R/R_w	0.0417/0.1150	0.0683/0.1791
Goodness-of-fit on F^2	0.896	1.009
(Δ/σ)max, mean	0.001, 0.000	0.001, 0.000
$\Delta\rho_{max}/\Delta\rho_{min}$ (e Å^{-3})	2.590 and −4.605	3.892 and −3.946

Yellow block crystals of **2** were obtained under similar reaction conditions, except that an equivalent amount of 2,2′-bipy was used in place of 4,4′-bipy.

2.3. *Structure determinations*

Suitable single crystals with dimension of 0.25 mm × 0.10 mm × 0.10 mm for **1** and 0.30 mm × 0.10 mm × 0.10 mm for **2** were carefully selected and glued on thin glass fibers with epoxy resin. Intensity data were collected on a Rigaku Mercury CCD diffractometer with graphite-monochromated Mo-Kα radiation ($\lambda = 0.71073$ Å). Empirical absorption corrections were performed using multi-scan. The structures were solved by direct methods and refined on F^2 by full-matrix least-squares using SHELX97 [26]. Anisotropic thermal parameters were applied to all nonhydrogen atoms. The organic hydrogens were generated geometrically. Crystallographic data are listed in table 1. Selected bond lengths and angles for **1** and **2** are listed in tables 2 and 3, respectively.

2.4. *Photocatalytic reaction*

Compound **1** (70 mg) was dispersed into a 70 mL RB (10 ppm) aqueous solution. Prior to irradiation, the mixture was magnetically stirred in the dark till the RB concentration was unchanged. Then the suspension was stirred and irradiated under a 500 W tungsten halogen lamp with a cut-off filter placed outside the Pyrex jacket to ensure irradiation with only visible light. The reaction was open to air and maintained at room

Table 2. Selected bond lengths (Å) and angles (°) for **1**.

W(1)–O(13)	1.651(9)	W(1)–O(10)	1.85(1)	W(1)–O(1)	1.88(1)
W(1)–O(3)	1.90(1)	W(1)–O(9)	1.90(1)	W(1)–O(21A)	2.48(1)
W(2)–O(14)	1.690(8)	W(2)–O(4)	1.86(1)	W(2)–O(12A)	1.863(9)
W(2)–O(2)	1.88(1)	W(2)–O(1)	1.88(1)	W(2)–O(21A)	2.43(1)
W(3)–O(15)	1.679(9)	W(3)–O(5)	1.872(9)	W(3)–O(9A)	1.90(1)
W(3)–O(11)	1.913(9)	W(3)–O(2)	1.93(1)	W(3)–O(19)	2.44(1)
W(4)–O(16)	1.668(9)	W(4)–O(7)	1.89(1)	W(4)–O(11A)	1.89(1)
W(4)–O(3)	1.90(1)	W(4)–O(6)	1.90(1)	W(4)–O(22)	2.53(1)
W(5)–O(17)	1.684(8)	W(5)–O(8)	1.86(1)	W(5)–O(6)	1.902(9)
W(5)–O(5)	1.91(1)	W(5)–O(4)	1.92(1)	W(5)–O(22)	2.44(1)
W(6)–O(18)	1.665(9)	W(6)–O(7)	1.89(1)	W(6)–O(12)	1.91(1)
W(6)–O(8)	1.92(1)	W(6)–O(10A)	1.92(1)	W(6)–O(22)	2.42(1)
V(1)–O(20A)	1.48(1)	V(1)–O(21A)	1.52(1)	V(1)–O(22)	1.55(1)
V(1)–O(19)	1.56(1)				
O(13)–W(1)–O(10)	102.4(5)	O(13)–W(1)–O(1)	103.9(6)	O(10)–W(1)–O(1)	89.0(4)
O(13)–W(1)–O(3)	101.7(6)	O(10)–W(1)–O(3)	155.7(6)	O(1)–W(1)–O(3)	88.1(5)
O(13)–W(1)–O(9)	99.4(6)	O(10)–W(1)–O(9)	84.8(5)	O(1)–W(1)–O(9)	156.6(6)
O(3)–W(1)–O(9)	88.4(4)	O(13)–W(1)–O(21A)	159.7(5)	O(10)–W(1)–O(21A)	64.1(5)
O(1)–W(1)–O(21A)	62.7(5)	O(3)–W(1)–O(21A)	93.3(6)	O(9)–W(1)–O(21A)	94.5(6)
O(14)–W(2)–O(4)	102.7(5)	O(14)–W(2)–O(12A)	101.2(5)	O(4)–W(2)–O(12A)	156.0(6)
O(14)–W(2)–O(2)	101.8(6)	O(4)–W(2)–O(2)	89.3(4)	O(12A)–W(2)–O(2)	87.2(4)
O(14)–W(2)–O(1)	101.6(6)	O(4)–W(2)–O(1)	87.2(5)	O(12A)–W(2)–O(1)	86.7(4)
O(2)–W(2)–O(1)	156.5(6)	O(14)–W(2)–O(21A)	158.9(5)	O(4)–W(2)–O(21A)	92.2(5)
O(12A)–W(2)–O(21A)	64.4(5)	O(2)–W(2)–O(21A)	93.1(5)	O(1)–W(2)–O(21A)	63.8(5)
O(15)–W(3)–O(5)	101.1(5)	O(15)–W(3)–O(9A)	103.5(6)	O(5)–W(3)–O(9A)	88.8(5)
O(15)–W(3)–O(11)	102.3(6)	O(5)–W(3)–O(11)	156.3(6)	O(9A)–W(3)–O(11)	89.3(4)
O(15)–W(3)–O(2)	100.6(5)	O(5)–W(3)–O(2)	86.7(5)	O(9A)–W(3)–O(2)	155.9(6)
O(11)–W(3)–O(2)	85.4(5)	O(15)–W(3)–O(19)	160.6(5)	O(5)–W(3)–O(19)	93.9(5)
O(9A)–W(3)–O(19)	64.3(5)	O(11)–W(3)–O(19)	64.1(5)	O(2)–W(3)–O(19)	92.4(5)
O(16)–W(4)–O(7)	103.8(5)	O(16)–W(4)–O(11A)	101.8(5)	O(7)–W(4)–O(11A)	86.9(5)
O(16)–W(4)–O(3)	100.4(6)	O(7)–W(4)–O(3)	155.8(6)	O(11A)–W(4)–O(3)	88.8(4)
O(16)–W(4)–O(6)	101.4(5)	O(7)–W(4)–O(6)	87.4(4)	O(11A)–W(4)–O(6)	156.9(6)
O(3)–W(4)–O(6)	87.3(5)	O(16)–W(4)–O(22)	158.3(5)	O(7)–W(4)–O(22)	62.3(5)
O(11A)–W(4)–O(22)	94.3(5)	O(3)–W(4)–O(22)	94.3(6)	O(6)–W(4)–O(22)	63.3(5)
O(17)–W(5)–O(8)	103.6(6)	O(17)–W(5)–O(6)	100.1(5)	O(8)–W(5)–O(6)	88.9(4)
O(17)–W(5)–O(5)	104.3(5)	O(8)–W(5)–O(5)	87.8(5)	O(6)–W(5)–O(5)	155.5(5)
O(17)–W(5)–O(4)	102.6(5)	O(8)–W(5)–O(4)	153.8(6)	O(6)–W(5)–O(4)	86.1(5)
O(5)–W(5)–O(4)	86.2(4)	O(17)–W(5)–O(22)	158.8(5)	O(8)–W(5)–O(22)	62.8(5)
O(6)–W(5)–O(22)	65.2(5)	O(5)–W(5)–O(22)	91.9(5)	O(4)–W(5)–O(22)	91.9(5)
O(18)–W(6)–O(7)	102.3(6)	O(18)–W(6)–O(12)	102.9(5)	O(7)–W(6)–O(12)	88.0(5)
O(18)–W(6)–O(8)	101.7(6)	O(7)–W(6)–O(8)	88.1(4)	O(12)–W(6)–O(8)	155.4(6)
O(18)–W(6)–O(10A)	103.5(6)	O(7)–W(6)–O(10A)	154.1(6)	O(12)–W(6)–O(10A)	88.2(4)
O(8)–W(6)–O(10A)	84.8(5)	O(18)–W(6)–O(22)	158.6(5)	O(7)–W(6)–O(22)	64.8(5)
O(12)–W(6)–O(22)	93.9(5)	O(8)–W(6)–O(22)	62.6(5)	O(10A)–W(6)–O(22)	90.0(5)
O(20A)–V(1)–O(21A)	112.0(7)	O(20A)–V(1)–O(22)	110.5(7)	O(21A)–V(1)–O(22)	110.2(7)
O(20A)–V(1)–O(19)	109.3(7)	O(21A)–V(1)–O(19)	108.6(7)	O(22)–V(1)–O(19)	106.0(7)

Symmetry codes: A: $-x+1, -y+1, -z$.

temperature by running cool water through an external coil. The RB concentration (C) was determined by the maximum absorbance at 554 nm as a function of irradiation time on a Spectrum lab 22PC.

2.5. *Preparation of 2-CPE*

Compound **2** was employed as a modifier to fabricate CPE (**2**-CPE) as the working electrode. Five hundred milligrams of graphite powder and 30 mg of **2** were mixed and ground together by an agate mortar and pestle to achieve an even, dry mixture.

Table 3. Selected bond lengths (Å) and angles (°) for **2**.

W(1)–O(13)	1.66(1)	W(1)–O(3)	1.90(2)	W(1)–O(2)	1.91(2)
W(1)–O(4)	1.92(1)	W(1)–O(1)	1.95(2)	W(1)–O(20A)	2.51(2)
W(2)–O(14)	1.68(1)	W(2)–O(11A)	1.80(1)	W(2)–O(1)	1.88(1)
W(2)–O(6)	1.87(1)	W(2)–O(5)	1.93(2)	W(2)–O(20A)	2.47(2)
W(3)–O(15)	1.65(1)	W(3)–O(7)	1.89(1)	W(3)–O(5)	1.90(2)
W(3)–O(8)	1.92(1)	W(3)–O(2)	1.93(2)	W(3)–O(20A)	2.37(2)
W(4)–O(16)	1.61(2)	W(4)–O(8A)	1.89(1)	W(4)–O(9)	1.89(1)
W(4)–O(3)	1.90(2)	W(4)–O(10)	1.92(2)	W(4)–O(22A)	2.50(2)
W(5)–O(17)	1.66(1)	W(5)–O(12A)	1.89(2)	W(5)–O(4A)	1.90(1)
W(5)–O(6)	1.90(1)	W(5)–O(10A)	1.92(20)	W(5)–O(19)	2.47(2)
W(6)–O(18)	1.70(2)	W(6)–O(7)	1.89(1)	W(6)–O(12)	1.89(2)
W(6)–O(9A)	1.91(1)	W(6)–O(11)	1.94(2)	W(6)–O(21)	2.41(2)
V(1)–O(22A)	1.49(3)	V(1)–O(21)	1.56(2)	V(1)–O(20A)	1.57(2)
V(1)–O(19)	1.57(2)				
O(13)–W(1)–O(3)	101.3(8)	O(13)–W(1)–O(2)	99.1(8)	O(3)–W(1)–O(2)	159.5(8)
O(13)–W(1)–O(4)	100.8(8)	O(3)–W(1)–O(4)	87.9(7)	O(2)–W(1)–O(4)	88.4(8)
O(13)–W(1)–O(1)	100.5(8)	O(3)–W(1)–O(1)	89.4(8)	O(2)–W(1)–O(1)	86.8(7)
O(4)–W(1)–O(1)	158.3(7)	O(13)–W(1)–O(20A)	157.0(7)	O(3)–W(1)–O(20A)	96.1(8)
O(2)–W(1)–O(20A)	64.3(8)	O(4)–W(1)–O(20A)	94.7(8)	O(1)–W(1)–O(20A)	64.5(7)
O(14)–W(2)–O(11A)	104.2(8)	O(14)–W(2)–O(1)	97.8(8)	O(11A)–W(2)–O(1)	89.2(8)
O(14)–W(2)–O(6)	104.7(7)	O(11A)–W(2)–O(6)	88.1(7)	O(1)–W(2)–O(6)	157.3(8)
O(14)–W(2)–O(5)	100.3(8)	O(11A)–W(2)–O(5)	155.7(9)	O(1)–W(2)–O(5)	87.5(7)
O(6)–W(2)–O(5)	85.7(8)	O(14)–W(2)–O(20A)	155.9(7)	O(11A)–W(2)–O(20A)	94.1(8)
O(1)–W(2)–O(20A)	66.4(8)	O(6)–W(2)–O(20A)	91.3(8)	O(5)–W(2)–O(20A)	62.6(8)
O(15)–W(3)–O(7)	100.9(7)	O(15)–W(3)–O(5)	101.6(8)	O(7)–W(3)–O(5)	157.4(8)
O(15)–W(3)–O(8)	100.5(7)	O(7)–W(3)–O(8)	86.8(5)	O(5)–W(3)–O(8)	86.7(7)
O(15)–W(3)–O(2)	100.9(8)	O(7)–W(3)–O(2)	88.3(6)	O(5)–W(3)–O(2)	89.9(7)
O(8)–W(3)–O(2)	158.6(8)	O(15)–W(3)–O(20A)	161.1(7)	O(7)–W(3)–O(20A)	93.6(7)
O(5)–W(3)–O(20A)	65.1(8)	O(8)–W(3)–O(20A)	92.2(7)	O(2)–W(3)–O(20A)	67.3(8)
O(16)–W(4)–O(8A)	102.2(7)	O(16)–W(4)–O(9)	103.0(8)	O(8A)–W(4)–O(9)	88.8(5)
O(16)–W(4)–O(3)	101.2(9)	O(8A)–W(4)–O(3)	156.6(8)	O(9)–W(4)–O(3)	87.5(6)
O(16)–W(4)–O(10)	99.3(9)	O(8A)–W(4)–O(10)	87.7(6)	O(9)–W(4)–O(10)	157.7(8)
O(3)–W(4)–O(10)	87.1(6)	O(16)–W(4)–O(22A)	160.2(9)	O(8A)–W(4)–O(22A)	66.0(7)
O(9)–W(4)–O(22A)	62.6(8)	O(3)–W(4)–O(22A)	91.9(9)	O(10)–W(4)–O(22A)	96.0(9)
O(17)–W(5)–O(12A)	101.5(8)	O(17)–W(5)–O(4A)	98.5(8)	O(12A)–W(5)–O(4A)	88.0(8)
O(17)–W(5)–O(6)	104.3(7)	O(12A)–W(5)–O(6)	87.7(8)	O(4A)–W(5)–O(6)	157.1(8)
O(17)–W(5)–O(10A)	99.6(8)	O(12A)–W(5)–O(10A)	158.8(8)	O(4A)–W(5)–O(10A)	87.4(7)
O(6)–W(5)–O(10A)	88.6(8)	O(17)–W(5)–O(19)	156.4(8)	O(12A)–W(5)–O(19)	95.5(8)
O(4A)–W(5)–O(19)	65.7(7)	O(6)–W(5)–O(19)	92.4(7)	O(10A)–W(5)–O(19)	63.8(8)
O(18)–W(6)–O(7)	102.9(7)	O(18)–W(6)–O(12)	103.5(9)	O(7)–W(6)–O(12)	88.3(7)
O(18)–W(6)–O(9A)	100.3(7)	O(7)–W(6)–O(9A)	88.3(5)	O(12)–W(6)–O(9A)	156.1(8)
O(18)–W(6)–O(11)	103.5(8)	O(7)–W(6)–O(11)	153.5(8)	O(12)–W(6)–O(11)	86.8(7)
O(9A)–W(6)–O(11)	85.7(6)	O(18)–W(6)–O(21)	160.2(8)	O(7)–W(6)–O(21)	92.4(7)
O(12)–W(6)–O(21)	63.9(8)	O(9A)–W(6)–O(21)	92.6(7)	O(11)–W(6)–O(21)	62.2(8)
O(22A)–V(1)–O(21)	116(1)	O(22A)–V(1)–O(20A)	109(1)	O(21)–V(1)–O(20A)	107(1)
O(22A)–V(1)–O(19)	112(1)	O(21)–V(1)–O(19)	108(1)	O(20A)–V(1)–O(19)	106(1)

Symmetry codes: A: $-x, -y+1, -z+1$.

Paraffin oil (0.22 mL) was then added to the mixture and stirred. The mixture was further packed into a graphite tube (3 mm inner diameter).

3. Results and discussion

3.1. *Description of crystal structures*

The single crystal X-ray crystallography of **1** and **2** reveal that they contain discrete $[VW_{12}O_{40}]^{4-}$. As shown in figures 1 and 2, a central VO_4 tetrahedron in $[VW_{12}O_{40}]^{4-}$ is

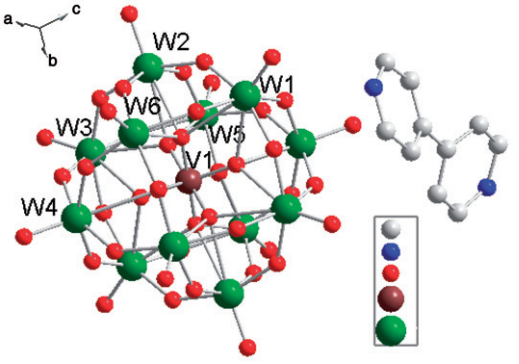

Figure 1. Ball and stick representation of **1**. All H atoms are omitted for clarity.

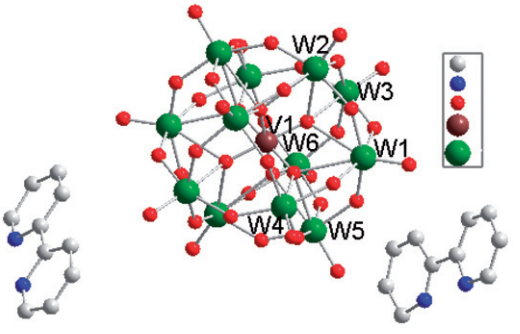

Figure 2. Ball and stick representation of **2**. All H atoms are omitted for clarity.

surrounded by 12 WO_6 octahedra that may be subdivided into four W_3O_{13} groups. Each W_3O_{13} group consists of three WO_6 octahedra linked in a triangular arrangement by sharing edges, and these four W_3O_{13} groups are linked together by sharing corners. The VO_4 tetrahedron is located at the center of the polyoxoanion by sharing its oxygens with four W_3O_{13} groups. All tungstens are VI oxidation state and have similar distorted octahedral environments defined by one terminal oxo-group with short W–O bond length (1.651–1.70 Å), four doubly bridging oxo-groups with intermediate W–μ_2-O bond lengths (1.80–1.93 Å), and one μ_4-oxygen (also bonded to V) with long W–μ_4-O distances (2.37–2.53 Å). The bond distances of W–O(t), W–O(μ_2) and W–O(μ_4) are in the normal range for $[XW_{12}O_{40}]^{n-}$ compounds [14–22]. The central V is surrounded by a cube of eight oxygens, with each oxygen site half-occupied. The O–V–O bond angles are in the range 106–116°. Average V–O distance is 1.54 Å, similar to the values reported for $[VW_{12}O_{40}][VO_2Ag(phen)_3]_2$ [21] and slightly shorter than the values for $[Me_4N]_7[VW_{12}O_{40}]\cdot 15H_2O$ [22]. The EPR spectrum recorded at 100 K on a crystalline sample of **1** is illustrated in figure 3. The hyperfine interaction $(2nI+1)$ line multiplets, where $n=1$ for a V(IV) center are observed with the ^{51}V nucleus ($I=7/2$) $g_{\|}=1.904$, $g_{\perp}=1.978$, $A_{\|}=191.8$G, and $A_{\perp}=68.6$G. The oxidation state of the central V is reduced (V^{IV}), in agreement with the charge balance of **1**.

Each $[VW_{12}O_{40}]^{4-}$ is surrounded by two $[4,4'\text{-}H_2bipy]^{2+}$ cations in **1** and four $[2,2'\text{-}Hbipy]^{+}$ in **2**. The $[4,4'\text{-}H_2bipy]^{2+}$ and $[VW_{12}O_{40}]^{4-}$ in **1** are connected into a 2-D

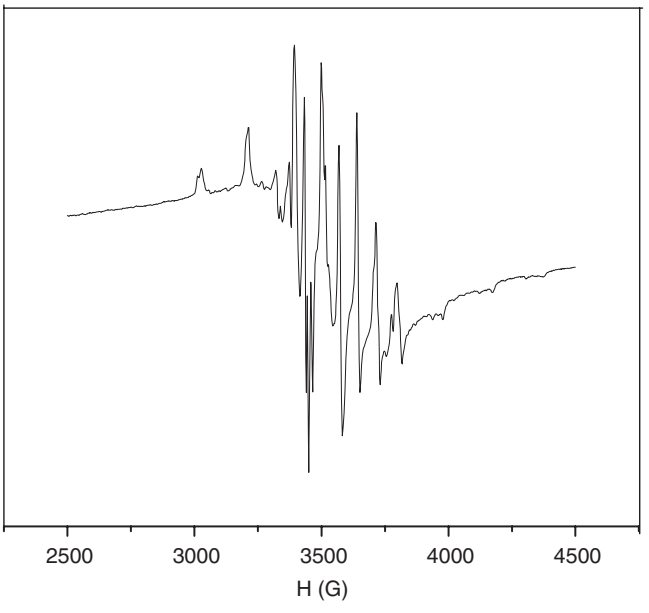

Figure 3. EPR spectrum of $[V_1W_{12}O_{40}]\cdot 2(4,4'\text{-}H_2bipy)\cdot 2H_2O$ at 100 K on a crystalline sample.

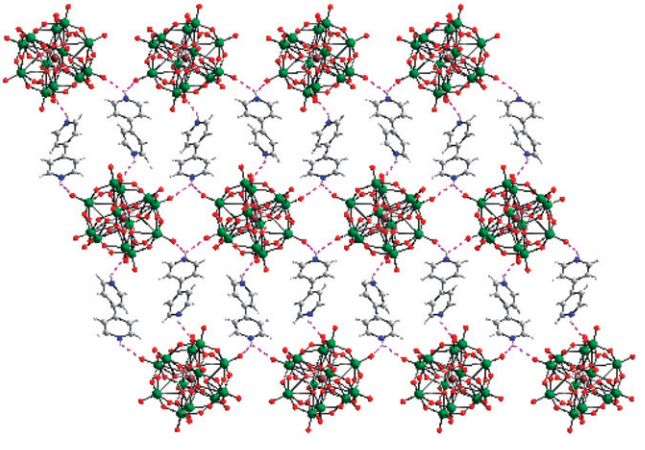

Figure 4. 2-D supramolecular architectures in **2**.

supramolecular network through tricentered hydrogen bonding (N2–H2B···O14 and N2–H2B···O17) and common hydrogen bonding (N1–H1B···O10) with distances of 2.81–3.07 Å (figure 4).

3.2. *IR spectrum*

Strong absorptions at 975 cm^{-1} for **1** and 968 cm^{-1} for **2** (figures S1 and S2) are combinations of ν(W–Ot). The bands near 801 and 887 cm^{-1} are assigned

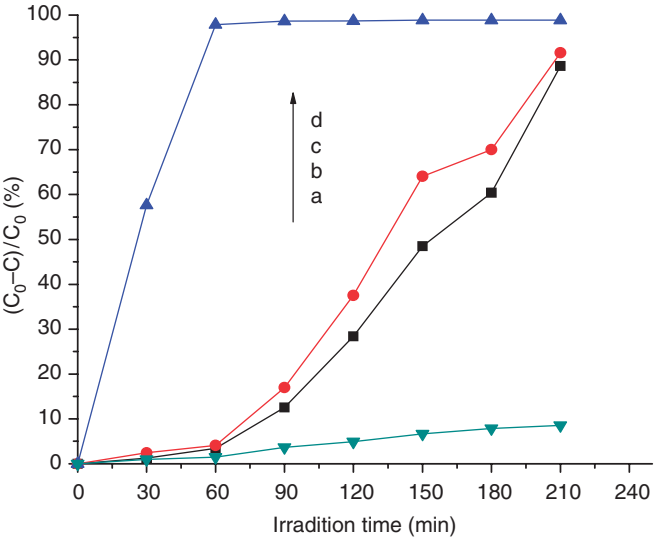

Figure 5. Decolorization rate of RB under different conditions (a) pH = 3.68, no catalyst; (b) pH = 2.78, POM; (c) pH = 4.38, POM; (d) pH = 1.48, POM.

to ν(W–Ob–W) and ν(W–Oc–W), and the peaks near 1069 cm^{-1} are associated with V–O vibration. Bands ranging from 1383 to 1630 cm^{-1} are characteristic of bipy [18].

3.3. *Thermal analysis*

TG curves of **1** and **2** indicate two steps of weight loss. In **1**, the first weight loss, 1.34% (Calcd 1.11%), at 80–320°C corresponds to release of lattice water; the second weight loss, 9.92% (Calcd 9.72%), between 320°C and 840°C is ascribed to decomposition of two bipy, 9.92% (Calcd 9.72%). In **2**, weight loss, 16.65% (Calcd 17.81%), at 300–860°C corresponds to decomposition of four bipy molecules.

3.4. *Photocatalytic activity of 1*

Owing to strong absorption in visible region and good stability under various pH conditions, RB was chosen as the primary dye pollutant to examine photo-decolorization behavior of **1** under visible irradiation. Decolorization of RB under different conditions is depicted in figure 5. There is no obvious decolorization of RB in the absence of **1**. Variation in pH greatly influences the photoassisted decolorization of RB. The decolorization rate of the RB increases on decreasing pH from 4.38 to 1.48 (figure 5b–d); decolorization of RB is 97% at pH 1.48 after 60 min, better than that of the reported POM [27, 28]. Thus, **1** may be a potential photocatalyst with high activity in reduction of some organic dyes.

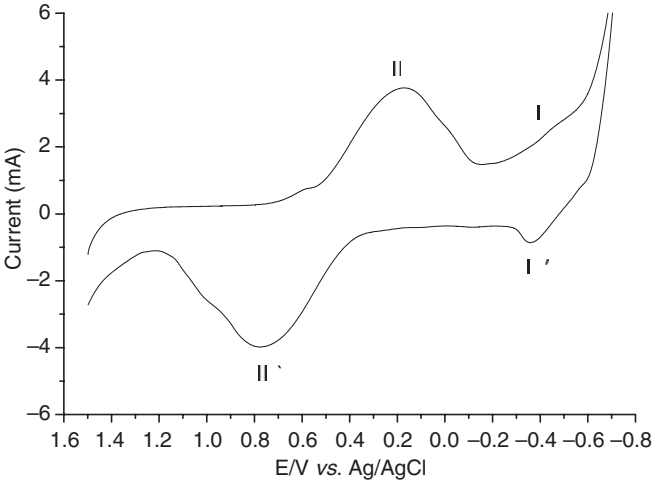

Figure 6. Cyclic voltammograms of **2**-CPE in the $Na_2SO_4 + H_2SO_4$ (pH = 1) solution. Scan rate: 100 mV s^{-1}.

3.5. *Electrochemical behavior of 2*

Figure 6 shows cyclic voltammetric behavior of the working electrode in $H_2SO_4 + Na_2SO_4$ aqueous solution (pH = 1). There are two redox waves, with E_p of −483 mV (I ~ I′) and 273 mV (II ~ II′) in the potential range −700 to +1500 mV. The former reduction peaks correspond to reduction of W^{VI} centers [29]. The latter reduction peaks correspond to reduction of V^{IV} centers [30].

As shown in figure 7, with the scan rate varying from 20 to 200 mV s^{-1}, the cathodic peak currents are almost the same as the corresponding anodic peak currents, and the peak potentials change gradually. The cathodic peak potentials shift to the negative direction and the corresponding anodic peak potentials shift to the positive direction with increasing scan rate. It should be pointed out that the peak-to-peak separation between the corresponding cathodic and anodic peaks increases with increasing scan rate [31]. Moreover, the peak current is proportional to the square root of the scan rate up to 200 mV s^{-1}, indicating diffusion controlled processes.

3.6. *Electrocatalytic activities of the 2-CPE on the reduction of H_2O_2*

Electrochemical reduction of H_2O_2 in water is of great interest due to its application in biosensors and fuel cells [32]. The direct reduction of H_2O_2 at bare carbon electrodes requires a high overpotential. The prepared **2**-CPE exhibits electrocatalytic reduction activity of H_2O_2 (figure 8). By increasing the concentration of H_2O_2, the cathodic peak current increases, while its anodic peak current decreases, clearly indicating that H_2O_2 is electrocatalytically reduced by $[VW_{12}O_{40}] \cdot 4(2,2'\text{-Hbipy})$ POM in **2**-CPE. Compound **2** exhibits good electrocatalytic activity for reduction of H_2O_2.

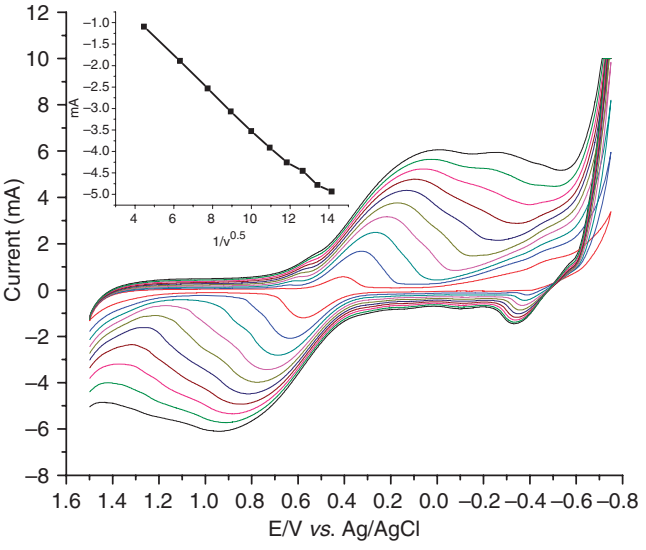

Figure 7. Cyclic voltammograms of **2**-CPE in the $Na_2SO_4 + H_2SO_4$ (pH = 1) solution at different scan rates (from inner to outer: 20, 40, 60, 80, ..., 200 mV s^{-1}). The inset shows the dependence of the cathodic peak current on the square root of the scan rate.

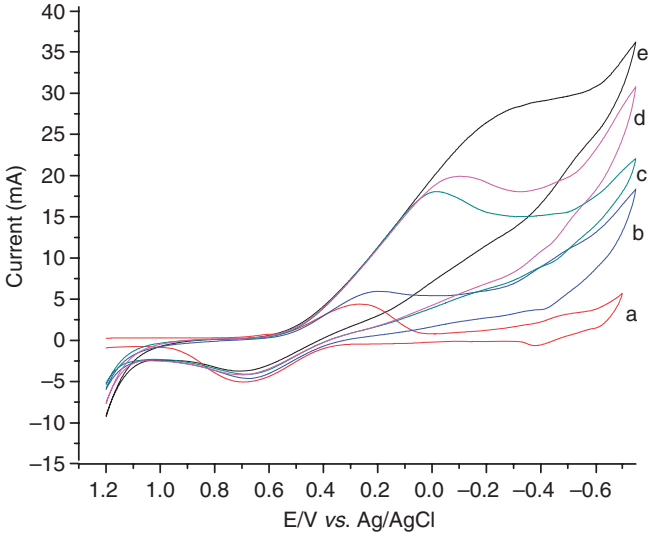

Figure 8. Cyclic voltammograms of **2**-CPE in the $Na_2SO_4 + H_2SO_4$ (pH = 1) solution at 100 mv s^{-1} (a) the absence of H_2O_2, (b) 5.0 mM H_2O_2, (c) 10.0 mM H_2O_2, (d) 15.0 mM H_2O_2, (e) 20.0 mM H_2O_2.

4. Conclusion

Two rare Keggin 12-tungstovanadate-bipyridine organic–inorganic hybrid compounds have been hydrothermally synthesized. In **1**, the protonated H_2bipy ligands and $[VW_{12}O_{40}]^{4-}$ form a 2-D supramolecular architecture by hydrogen-bonding.

Compound **1** exhibits effective photocatalytic activity for degradation of RB solution and **2** shows good catalytic activity for reduction of hydrogen peroxide, showing Keggin 12-tungstovanadate-bipyridine organic–inorganic hybrids have potential application in photocatalysis and electrochemical sensors.

Supplementary material

Crystallographic data have been deposited in the Cambridge Crystallographic Center with CCDC Nos. 699030 and 699028. Supplementary data are available from The Director, CCDC, 12 Union Road, Cambridge, CB2 1EZ, UK (Fax: +44-1223-336033; E-mail: deposit@ccdc.cam.ac.uk; www: http://www.ccdc.cam.ac.uk) on request.

Acknowledgements

This project was financially supported by the National Natural Science Foundation of China (No. 20771024) and the Natural Science Foundation of Fujian Province (No. 2008J0142).

References

[1] H. Jin, C. Qin, Y.G. Li, E.B. Wang. *Inorg. Chem. Commun.*, **9**, 482 (2006).
[2] A. Tripathi, T. Hughbanks, A. Clearfield. *J. Am. Chem. Soc.*, **125**, 10528 (2003).
[3] D. Hagrman, J. Zubieta. *J. Chem. Soc., Chem. Commun.*, 2005 (1998).
[4] C.M. Liu, D.Q. Zhang, M. Xiong, D.B. Zhu. *J. Chem. Soc., Chem. Commun.*, 1416 (2002).
[5] Y. Ishii, Y. Takenaka, K. Konishi. *Angew. Chem., Int. Ed.*, **43**, 2702 (2004).
[6] H.Y. An, E.B. Wang, D.R. Xiao, Y.G. Li, Z.M. Su, L. Xu. *Angew. Chem. Int. Ed.*, **45**, 904 (2006).
[7] M.T. Pope, A. Muller. *Angew. Chem., Int. Ed. Engl.*, **30**, 34 (1991).
[8] E. Gkika, A. Troupis, A. Hiskia, E. Papaconstantinou. *Appl. Catal. B: Environ.*, **62**, 28 (2006).
[9] C.C. Chen, Q. Wang, P.X. Lei, W.J. Song, W.H. Ma, J.C. Zhao. *Environ. Sci. Technol.*, **40**, 3965 (2006).
[10] C.L. Hill. *J. Mol. Catal. A*, **262**, 2 (2007).
[11] L. Cheng, G.E. Pacey, J.A. Cox. *Electrochim. Acta*, **46**, 4223 (2001).
[12] M. Jiang, X.D. Zhai, M.H. Liu. *J. Mater. Chem.*, **17**, 193 (2007).
[13] Y.C. Li, W.F. Bu, L.X. Wu, C.Q. Sun. *Sens. Actuators B*, **107**, 921 (2005).
[14] T.H. Li, J. Lu, S.Y. Gao, R. Cao. *Inorg. Chem. Commun.*, **10**, 551 (2007).
[15] J.M. Knaust, C. Inman, S.W. Keller. *Chem. Commun.*, 492 (2004).
[16] H.L. Chen, Y. Ding, X.X. Xu, E.B. Wang, W.L. Chen, S. Chang, X.L. Wang. *J. Coord. Chem.*, **62**, 347 (2009).
[17] W.L. Huang, L. Todaro, G.P.A. Yap, R. Beer, L.C. Francesconi, T. Polenova. *J. Am. Chem. Soc.*, **126**, 11564 (2004).
[18] J.Y. Niu, Y. Shen, J.P. Wang. *J. Mol. Struct.*, **733**, 19 (2005).
[19] J.L. Xie. *J. Coord. Chem.*, **61**, 3993 (2008).
[20] M.X. Li, G.L. Guo, J.Y. Niu. *J. Coord. Chem.*, **61**, 2896 (2008).
[21] M.X. Yang, S. Lin, L.J. Chen, X.F. Zhang, H.H. Xu. *Inorg. Chem. Commun.*, **12**, 566 (2009).
[22] M.I. Khan, S. Cevik. *J. Chem. Soc., Dalton Trans.*, 1651 (1999).
[23] Y.H. Guo, D.F. Li, C.W. Hu. *Appl. Catal. B: Environ.*, **30**, 337 (2001).
[24] L.A. Glinskaya, É.N. Yurchenko, R.F. Klevtsova, L.V. Derkach, A.M. Rios, T.P. Lazarenko. *J. Struct. Chem.*, **30**, 427 (1989).
[25] R.F. Klevtsova, L.A. Glinskaya, É.N. Yurchenko, T.D. Gutsul. *J. Struct. Chem.*, **32**, 687 (1991).

[26] (a) G.M. Sheldrick, *SHELX 97, Program for Crystal Structures Refinement*, University of Göttingen, Germany (1997); (b) G.M. Sheldrick, *SHELX 97, Program for Crystal Structures Solution*, University of Göttingen, Germany (1997).
[27] X.Q. Chen, S. Lin, L.J. Chen, X.H. Chen, C.L. Liu, J.B. Chen, L.Y. Yang. *Inorg. Chem. Commun.*, **10**, 1285 (2007).
[28] B.Z. Lin, X.Z. Liu, B.H. Xu, Q.Q. Wang, Z.J. Xiao. *Solid State Sci.*, **10**, 1517 (2008).
[29] S.Y. Gao, X. Li, C.P. Yang, T.H. Li, R. Cao. *J. Solid State Chem.*, **179**, 1407 (2006).
[30] B. Keita, L. Nadjo. *J. Mol. Catal. A: Chem.*, **262**, 190 (2007).
[31] H. Jin, Y.F. Qi, D.R. Xiao, X.L. Wang, S. Chang, E.B. Wang. *J. Mol. Struct.*, **837**, 23 (2007).
[32] F. Matsumoto, S. Uesugi, N. Koura, T. Ohsaka. *J. Electroanal. Chem.*, **549**, 71 (2003).